PPPL-3301, Preprint: May 1998, UC-426

Design Study of a Visible/Infrared Periscope for Intense Radiation Applications using Reflective Optics

S. S. Medley

Princeton Plasma Physics Laboratory, P. O. Box 451, Princeton, NJ 08543 USA

Abstract

In magnetically-confined fusion devices employing deuterium-tritium operation, refractive optical components exposed to neutron and gamma radiation can be subject to degradation of the transmission characteristics, induced luminescence, and altered mechanical properties including dimensional changes. Although radiation resistant refractive optics functioned well for the TFTR periscope system during D-T operation, this design approach is unpromising in the much more hostile radiation environment of future D-T devices such as ITER. Under contract to the Princeton Plasma Physics Laboratory, Ball Aerospace of Colorado carried out a periscope design study based on the use of reflective optics. In this design, beryllium reflective input optics supported by a fused silica optical bench were interfaced to a Cassegrain relay system to transfer plasma images to remotely located cameras. This system is also capable of measuring first-wall surface temperatures in the range of 300 °C - 2000 °C even under projected heating of the reflective optics themselves to several hundred degrees Celsius. Tests of beryllium mirror samples, however, revealed that operation at temperatures above 700 °C leads to a loss of specular reflectivity, thus placing an upper limit on the acceptable thermal environment. The main results of this periscope study are presented in this paper.

I. INTRODUCTION

The study by Ball Aerospace of a periscope concept using reflective optical components was initiated by the Princeton Plasma Physics Laboratory (PPPL) as part of diagnostic development[1] for the Compact Ignition Tokamak (CIT) design project and was subsequently incorporated in the diagnostic plans[2] for the design of the Tokamak Physics Experiment. The periscope system is to be used for internal inspection of the vacuum vessel, imaging the plasma and divertor regions during operation and infrared measurement of the surface temperature of the first wall structures. With regard to performance, the periscope is required to have a wide angle view of the interior of the vacuum vessel with resolutions on the order of 10^{-3} to 10^{-2}. Routine maintenance, re-alignment or replacement of components would need to be performed using remote handling techniques and therefore should be avoided. The problem with refractive optical approaches is radiation damage: unhardened glass begins to show damage at 10^4 rads, fused silica and glasses hardened with cerium oxide degrade 10 - 20 percent at 10^7 rads. The typical radiation dose rates expected in diagnostic applications involving DT operation are in excess of 10^4 rads^{-1} which would entail replacement of refractive optical components several times over the lifetime characteristic of such experiments.

The periscope operational environment was based on design characteristics of the CIT machine. The environment consists of high temperature blackbody radiation (T ~ 1.8×10^8 °K), x-rays and gamma rays (~ 120 Wcm^{-2}), a large flux of 14 MeV neutrons (~ 10^{15} cm^{-2}s^{-1} or a dosage rate of ~ 10^6 rads^{-1}), a high magnetic field (B ~ 6 T) with large disruption-induced slew rates (dB/dt ~ 200 Ts^{-1}) and contamination from wall material (mainly carbon). Furthermore, those components nearest the plasma may have to endure and operate over temperature variation of several hundred degrees Celsius. During the 13 s CIT pulse, the surface temperature of the first wall structures is expected to rise from the 350 °C ambient to a level of ~ 2000 °C. Continuous, real time measurement of the heating and cooling cycle of these components is required with a spatial resolution of about 1 cm^2. The tile emissivity can range from 0.7 - 0.8 < 2000 °C and rise to 0.9 for higher temperatures.

The purpose of this paper is to present an overview of the salient results contained in the limited-distribution reports[3-6] on the refractive optic periscope design prepared by Ball Aerospace for PPPL.

II. PERISCOPE DESIGN

A brief survey of periscope design approaches by Ball Aerospace discarded diffractive optics and tube optics. The diffractive approach was eliminated because of doubtful survivability of the gratings or zone plates in the operating environment and tube optics (hollow, cylindrical light guides) were disadvantaged by low throughput and resolution. In the design approaches examined for the optical periscope system for CIT, a general finding was that systems with good optical performance were complex and at high risk of failure while simpler robust systems returned inferior optical performance. The concept adopted was a periscope system based on reflective optics and a study of candidate materials was performed.

Nuclear heating of candidate materials was examined since the heating of periscope components can present a serious problem to performance. Neutrons and gamma radiation are very penetrating and for material thicknesses characteristic of this application the kinetic energy released by this source results in bulk energy deposition. In contrast to neutron and gamma radiation, x-rays are primarily adsorbed in the surface layers and contribute to surface heating and temperature gradients in the absorbing material.

The bulk and surface heating calculated for selected materials are listed in Table 1 and plotted in Fig. 1. The last row in Table 1 gives the bulk heating due to neutrons and gamma radiation. The interaction rate for this radiation can be considered uniform for the material thicknesses relevant to the periscope design. The bulk heating was obtained by multiplying the numerically calculated kerma (kinetic energy released in materials) for selected materials at the periscope port location of CIT[9] by the density of the element. For compound materials, the bulk heating was obtained by summation over the kerma rates and fractional densities of the individual elements. The remainder of Table 1 gives the energy deposition due to x-rays which are primarily absorbed in the surface layers and contribute to surface heating and temperature gradients in the absorbing material. This study led to the choice of beryllium for reflective optical components, since the combined bulk and surface heating of Be is lower than all the other materials examined.

Table 1 Energy Deposition (Wcm^{-3}) in Candidate Periscope Materials

Penetration Depth (cm)	Beryllium (Be)	Alumina (Al_2O_3)	Tungsten Carbide (WC)	Beryllia (BeO)	Silicon Carbide (SiC)	Silica (SiO_2)
10^{-4}	17.20	629	6940	145	508	370
10^{-3}	13.76	393	3260	109	323	243
10^{-2}	10.33	197	1220	65	169	137
10^{-1}	6.536	86.5	196	33	77	63
10^{0}	2.924	16.1	7.34	12	15.4	16
10^{1}	1.135	1.18	1.8	1.5	1.5	1.6
Bulk	38.3	52.6	268	52.5	39.5	33.5

The general design concept adopted for a periscope using beryllium reflective optics is as follows. The desire for a field of view which encompassed the midplane the divertor region leads to a requirement for a wide angle system having approximately 70° FOV as illustrated in Fig. 2. In order to provide this wide field of view of the vessel interior, mirrors were positioned deep within the diagnostic access port by means of a cantilevered optical bench to form a virtual image of the vessel interior. Two mirrors in a periscope arrangement were needed: a convex spherical mirror and a flat mirror as shown by the detail in Fig. 2. A fused silica tube, the optical bench, is cantilevered through the horizontal port and supports the forward two optics of the system at the mouth of the port. The optical bench is a tube of circular cross section concentric with the optical axis of the system and is supported on a pair of ceramic ball bearing rings enabling it to rotate around its long axis, thus scanning the field of view about the chamber interior. Versatility can be further increased by telescoping the bench and articulating the mirrors so that point-of-view as well as field-of-view can be varied and the mirrors can be stowed facing away from the plasma if desired. The vacuum seal at the port flange is made using a reentrant bellows which allows for motion of the vacuum vessel during plasma operation and vessel bakeout.

The optical path passes from the forward mirrors through the interior of the tube to a folding mirror which reflects the path down to the vacuum window located out of the direct radiation streaming flux through the port. The resulting image was relayed to remotely located cameras by a series of afocal Cassegrain relays wherein each relay stage is composed of two (paired) confocal eccentric pupil Cassegrain telescopes. This design is correctable for a wide range of aberrations and field curvature is controlled by making the radii of curvature of the primary and secondary mirrors identical. The first telescope is designed to work between finite conjugates, relaying the virtual image formed by the internal convex mirror to the confocal image plane. Relay stages are used successively to attain the needed distance, each one adding about five meters. Flat folding mirrors are placed as necessary between stages to lead the relay along the desired path. A final stage must be provided to match the image to a detector.

With rotation of the periscope optics around the input axis, of order 1/3 of the vacuum vessel interior could be viewed from a single horizontal access port. However, ray tracing analysis showed that a single, wide-angle (~ 70°) aperture system results in a periscope that is extremely slow with relatively low resolution. Another approach is use separate optical systems with reduced fields of view. For example, one system could be a 22° high resolution periscope to observe the divertor region with ~ 1 mm resolution while another 40° by 60° system would view the entire plasma at low speed with ~ 10 mm resolution. In pursuing this approach, a further improvement was realized by making the turning mirror cylindrical, rather than flat to correct some of the astigmatism introduced by the tilted spherical first mirror. Ray tracing analysis was performed for the 40-60° system with an aperture of 75 mm. The system operates at F/17 at the first image plane. The corresponding solid angle is about 3.0×10^{-3} steradians, which with an image area of 533 mm^2 gives an area-solid angle product of $A\Omega = 2.1\ mm^3 ster$ and a resolution of ~ 10-15 mm. Another ray trace analysis was done with a 22° view center on 51° from the centerline of the access port with an aperture of 75 mm operating at F/17 as before, resulting in a resolution of ~ 2 mm. However, the work to advance the design of shared aperture systems to the point were they can be evaluated for operational suitability and manufacturability was not part of this study.

III. INFRARED PERFORMANCE

The feasibility of performing thermal radiometric measurement of the temperature of the first wall structures inside the vacuum vessel using the periscope concept based on beryllium reflective optics was examined. As a result of absorption of energy emitted from the plasma, the first and second mirrors of the periscope were estimated to rise to temperatures of around 700 °C during the 13 s discharge duration followed by cooling that could range down to the 350 °C environment between pulses. The effect of the elevated mirror temperatures on the accuracy of the tile temperature measurement was a concern in the design study. Preliminary calculations performed at various pass bands in the wavelength range from 1 - 10 microns indicated that ample temperature-dependent signal was available, so operation at shorter wavelengths was pursued. The analysis revealed that not only was it feasible to operate at wavelengths below one micron, but substantial improvement in accuracy of tile temperature measurement is also achieved.

For analysis simplicity, it was assumed that the optical match assured that all of the flux within the field-of-view acceptance angle falls on the detector, regardless of focal length. The latter will determine system magnification and F/# but will not affect the pixel power since it depends only on the system $A\Omega$ and the transmission of the optics. Using conventional analysis methods for a Lambertian radiator viewed at normal incidence, the radiant flux or power collected by a 1 cm^2 tile area (assumed to be one meter from the entrance pupil) on a single pixel at the focal plane, $P_{tile}(T)$, is given by:

$$P_{tile}(T) = \varepsilon_t \frac{M(T)}{\pi} A\Omega (R_{be})^2 T_{op} \qquad (1)$$

and the pixel background flux at the focal plane from the mirror heat, $P_{Be}(T)$, is:

$$P_{Be}(T) = \varepsilon_{Be} \frac{M(T)}{\pi} A\Omega T_{op} \qquad (2)$$

where R_{be} = reflectivity of the Be mirrors

T_{op} = transmission of the optical train after the mirrors

ε_t = tile emissivity

ε_{Be} = Be mirror emissivity

$A\Omega$ = area-solid angle product

and the tile radiant emittance, M(T), is given by:

$$M(T) = \int \frac{2\pi hc^2}{\lambda^5 \left(e^{hc/\lambda kT} - 1\right)} d\lambda \quad \mathrm{Wcm^{-2}} \qquad (3)$$

where the integral is over the wave length range of the selected pass band.

Plots of the tile pixel power (solid symbols) as a function of temperature are shown in Fig. 3, along with the apparent tile power (open symbols) resulting from heated mirrors assumed to be at a temperature of 895 °K. The parameters values used were R_{be} = 0.4, T_{op} = 0.1, ε_t = 0.8, ε_{Be} = 0.4 and results are shown for two pass bands: 0.1 -1 μ and 1 - 2 μ. Clearly, the accuracy of determining the tile temperature rapidly deteriorates at and below the mirror temperature. The ΔT equivalent between the actual and apparent tile temperature is shown in Fig. 4 for the two pass bands used. A dramatic difference between the two pass bands is evident; the temperature error due to the mirror background is significantly smaller for the shorter wavelength case. In the event that a measure of the evolution of the mirror temperature is available, corrections could be made to significantly improve the accuracy of the tile temperature measurement. Under actual experimental conditions, out-of-band rejection filters will be needed to exclude power from extraneous sources reaching the detectors.

IV. BERYLLIUM MIRROR EVALUATION

Thermal analysis predicted that the maximum temperatures for the Be mirrors would approach 700 °C with very small front-to-back gradients (~ 2 °C). However, this analysis can not accurately predict the temperature at depths of less than 10 nm where it might be considerably higher. The visible light reflectance of Be is low; on the order of 40% - 50% and possibility that this might be further reduced in the envisioned operating environment needed to be addressed.

A bare beryllium surface is know to be highly reactive, oxidizing rapidly even at room temperature. In operation, the beryllium mirrors will be subjected to temperatures ranging from room temperature to ~ 900 °C and to oxygen doses up to 1500 Langmuirs (1 L = 1×10^{-6} Torr-sec). According to previous results in the literature[10], under these conditions and without prior removal of the native oxide, oxidation proceeds at a very low rate and the loss of specular reflectivity results not from an increase in the oxide thickness, but from a roughening of the surface on a micron scale which coincides with a depletion of the surface oxide. The objective of the present study was to verify this expectation for the particular type of mirror samples of interest.

The oxidation rates of a beryllium mirror surface were measured as a function of temperature and oxygen dose at the Colorado School of Mines[6] using Auger Electron Spectroscopy (AES) in ultra-high vacuum. Small Be coupons (0.394" squares of 0.125" thickness) optically polished to a $\lambda/4$ flatness were inserted into a machinable ceramic (aluminum silicate) holder with an embedded tungsten filament for heating of the sample. Starting with the native oxide surface, the sample was heated in a vacuum environment of ~ 10^{-9} Torr and the oxide thickness was deduced at various temperatures from the ratios of the BeO peaks to that of pure Be metal observed in the Auger spectra. In this way, the native oxide thickness was determined to be ~ 30 Angstroms. The reflectivity was obtained qualitatively by visual observation. As the sample was heated to 900 °C, the native oxide thickness was observed to decrease to about 13 Angstroms, as shown be the experimental results in Fig. 5. A change in the slope at 700 °C can be seen in the plot, at which point the Be surface was observed to roughen and the visual reflectivity started to degrade. Oxygen dosing at an oxygen partial pressure of 10^{-6} Torr at various temperatures up to 800 °C yielded the same behavior as the native oxide sample; i.e. a loss of specular reflectivity occurred at temperatures of 700 °C and above regardless of oxygen dose. Annealing at 600 °C for a period of 72 hours produced no change in either the Auger spectrum or the specular reflectivity.

V. SUMMARY

A periscope design based on the use of beryllium reflective optics appears to provide a visible/infrared optical system that is robust in a hot radiation and thermal environment. It appears basically feasible to use the periscope optical system for thermal radiometry. The preferred spectral region for this radiometry turns out to be in the visible rather than the infrared because this choice reduces the tile temperature errors due to the hot mirrors.

The major finding of the beryllium mirror evaluation was that heating of the Be samples to temperatures of 700 °C and above produces structural changes in the surface which leads to a loss of specular reflectivity, rendering the material virtually useless as an optical mirror. These changes appear to be correlated with a *decrease* in surface oxide thickness. Oxygen dosing of the surface produced no detectable increase in the oxide thickness or additional degradation of the reflectivity at any temperature up to the maximum investigated (900 °C).

ACKNOWLEDGMENT

This work was supported by US DoE Contract DE-AC02-76CH03073

REFERENCES

1 S. S. Medley and K. M. Young, "Plasma Diagnostics for the CIT," Rev. Sci. Instrum. **59**, 1745 (1988).

2 S. S. Medley, "Tokamak Physics Experiment Diagnostic Plans," Rev. Sci. Instrum. **66**, 297 (1995).

3 "Study of Remote Stable Optical Systems for the Compact Ignition Tokamak," Ball Aerospace Report F88-05 (July, 1988).

4 "Ray Trace Design Study of Optical Systems for the Compact Ignition Tokamak," Ball Aerospace Report F89-03-1 (January, 1989).

5 "Thermal Radiometry Study for the Compact Ignition Tokamak," Ball Aerospace Report F88-03-2 (February, 1989).

6 "Beryllium Mirror Study for the Compact Ignition Tokamak," Ball Aerospace Report F89-03-3 (June, 1989).

7 F. W. Clinard, Jr., E. H. Farnum, D. L. Griscom, R. F. Mattas, S. S. Medley, F. W. Wiffen, S. S. Wojtowicz, K. M. Young and S. J. Zinkle, J. Nucl. Mater. **191-194**, 1403 (1992).

8 S. S. Medley, D. L. Dimock, S. Hayes, D. Long, J. L. Lowrance, V. Mastrocola, G. Renda, M. Ulrickson and K. M. Young. Rev. Sci. Intrum. **56**, 1873 (1985).

9 S. L. Liew and L. P Ku, "An assessment of the CIT Radiation Environment Using Coupled Three-Dimensional and Reduced Transport Models," IEEE Proceedings of the 12th Symposium on Fusion Engineering, October 1997, IEEE Catalog No. 87CH2507-2, p 1548.

10 Thermophysical Properties of Matter, ed. Y. S. Touloukian, The TPRC data series.

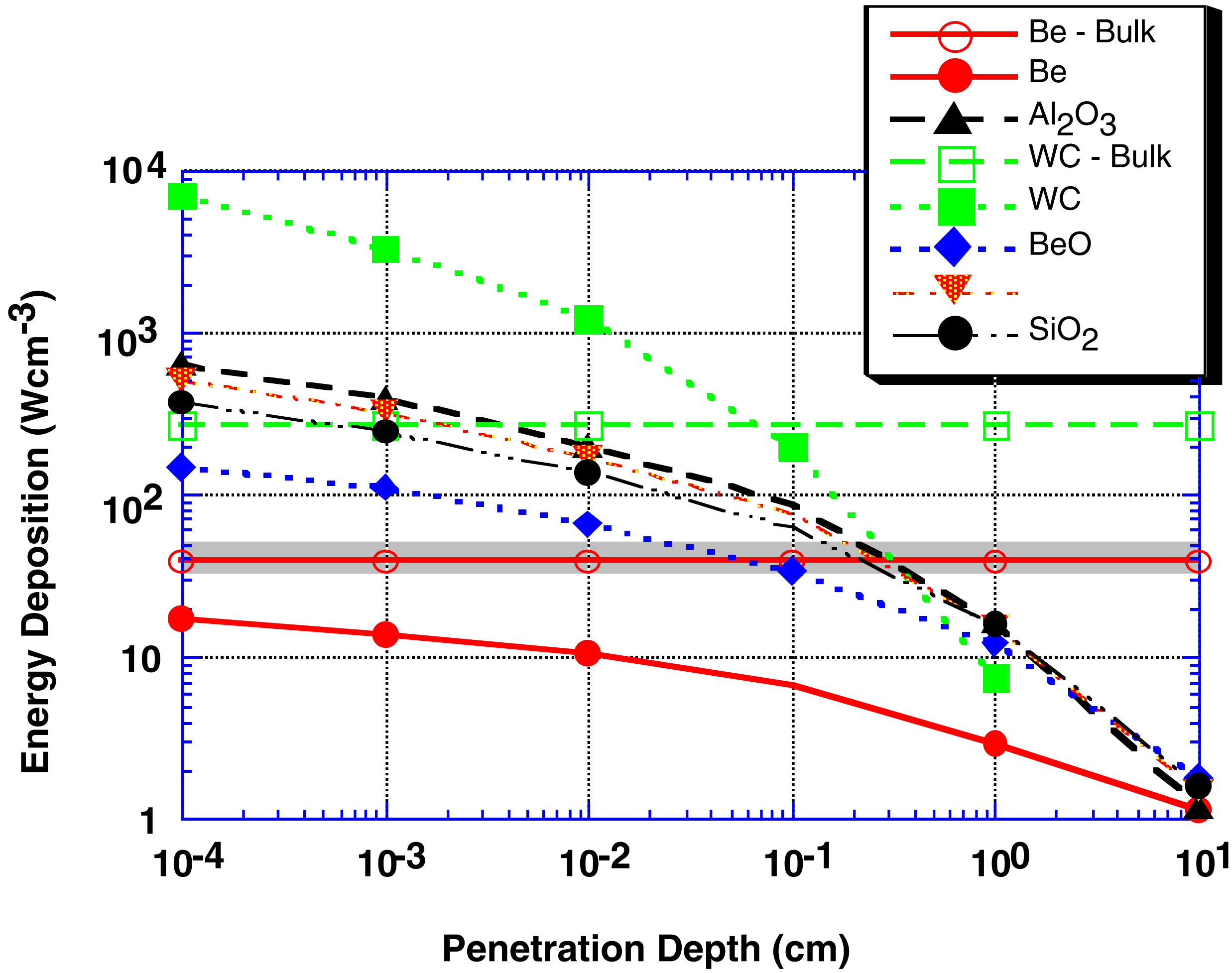

Fig. 1 Energy deposition in candidate periscope materials due to "bulk" heating by neutrons and gamma radiation (curves) and "surface" heating due to x-rays (horizontal lines). The surface heating for all materials other than Be and tungsten carbide (WC) lie within the hatched band.

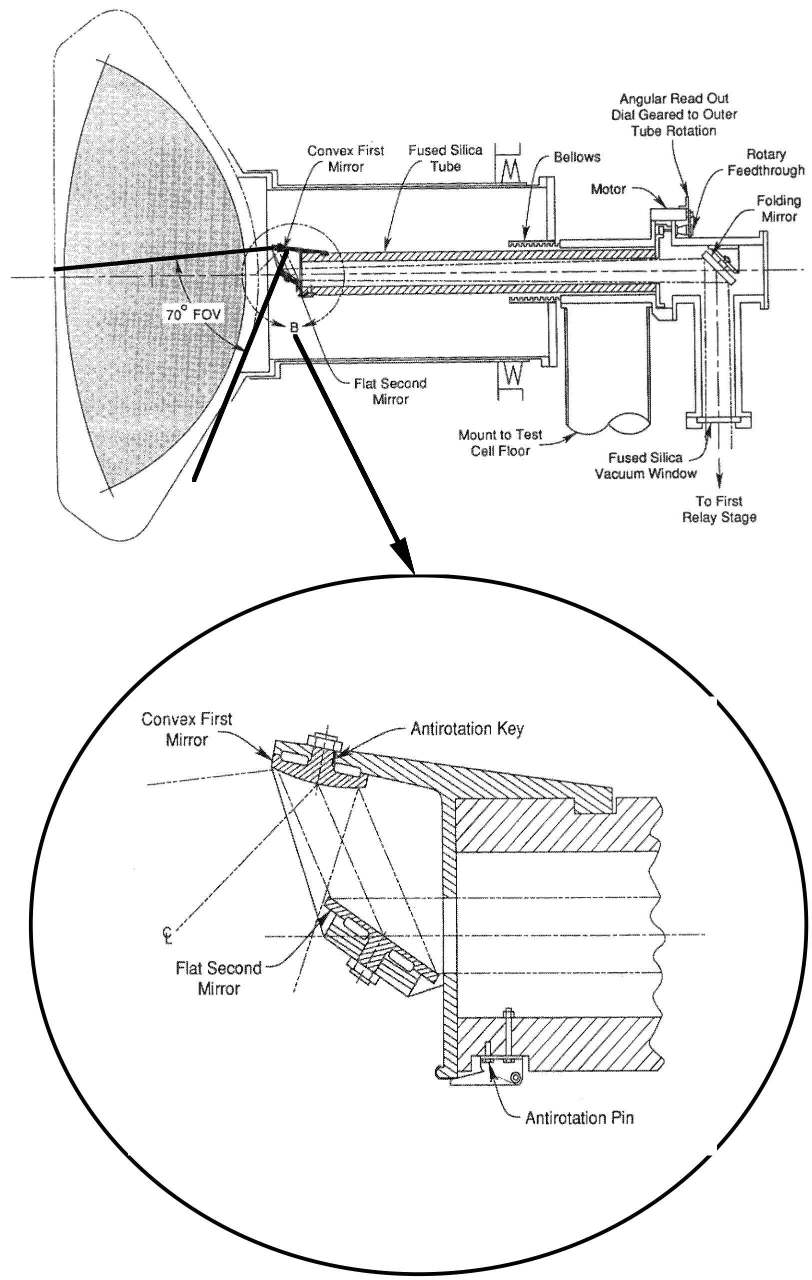

Fig. 2 Elevation view of a periscope concept developed for PPPL by Ball Aerospace, Colorado. Beryllium reflective input optics which are supported by a fused silica "optical bench" are interfaced to a Cassegrain relay system to transfer plasma images to remotely located cameras. The bottom panel shows detail of the collection optical elements.

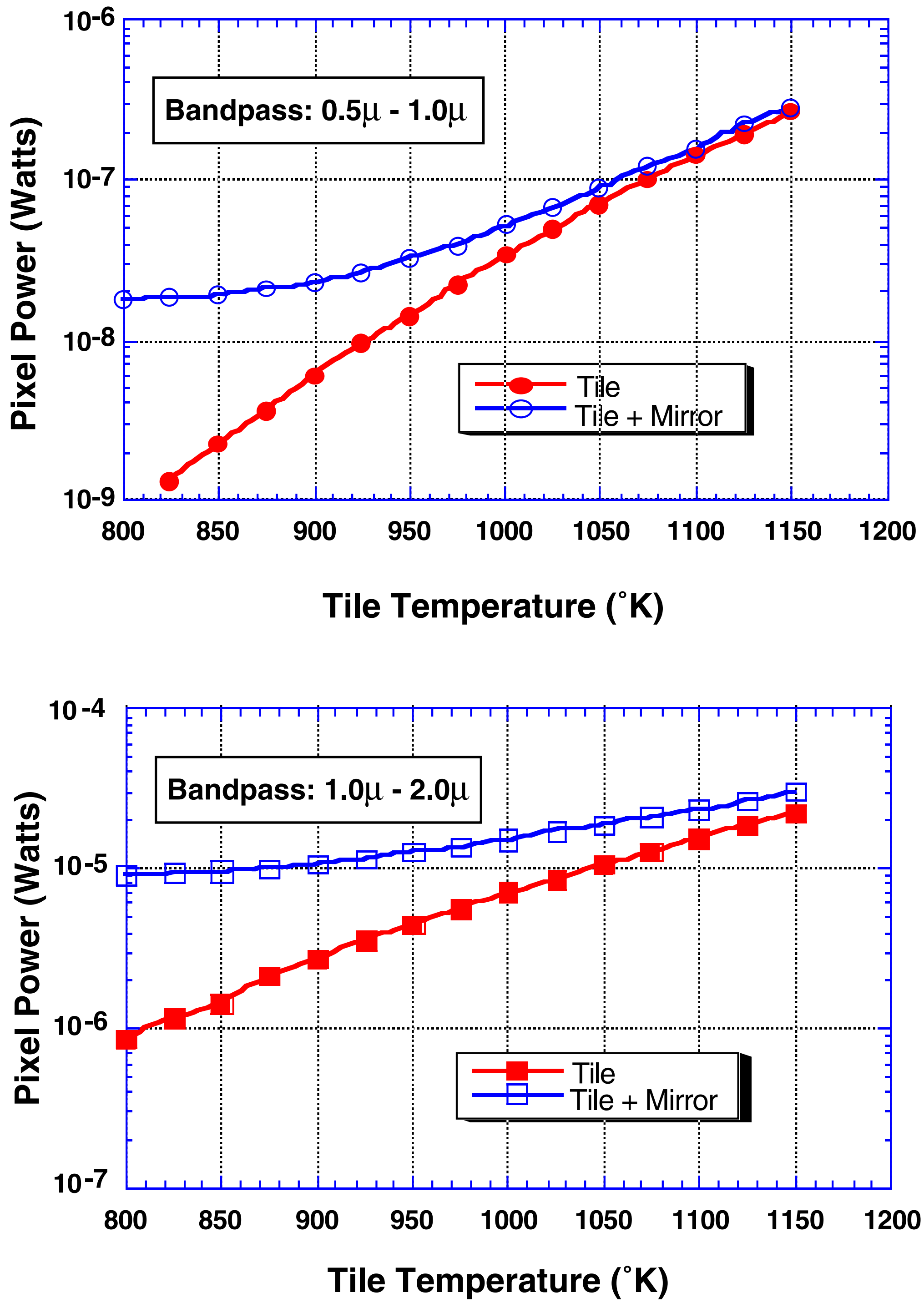

Fig. 3 Analysis of Be periscope performance for infrared measurements of the vacuum vessel first wall structures.

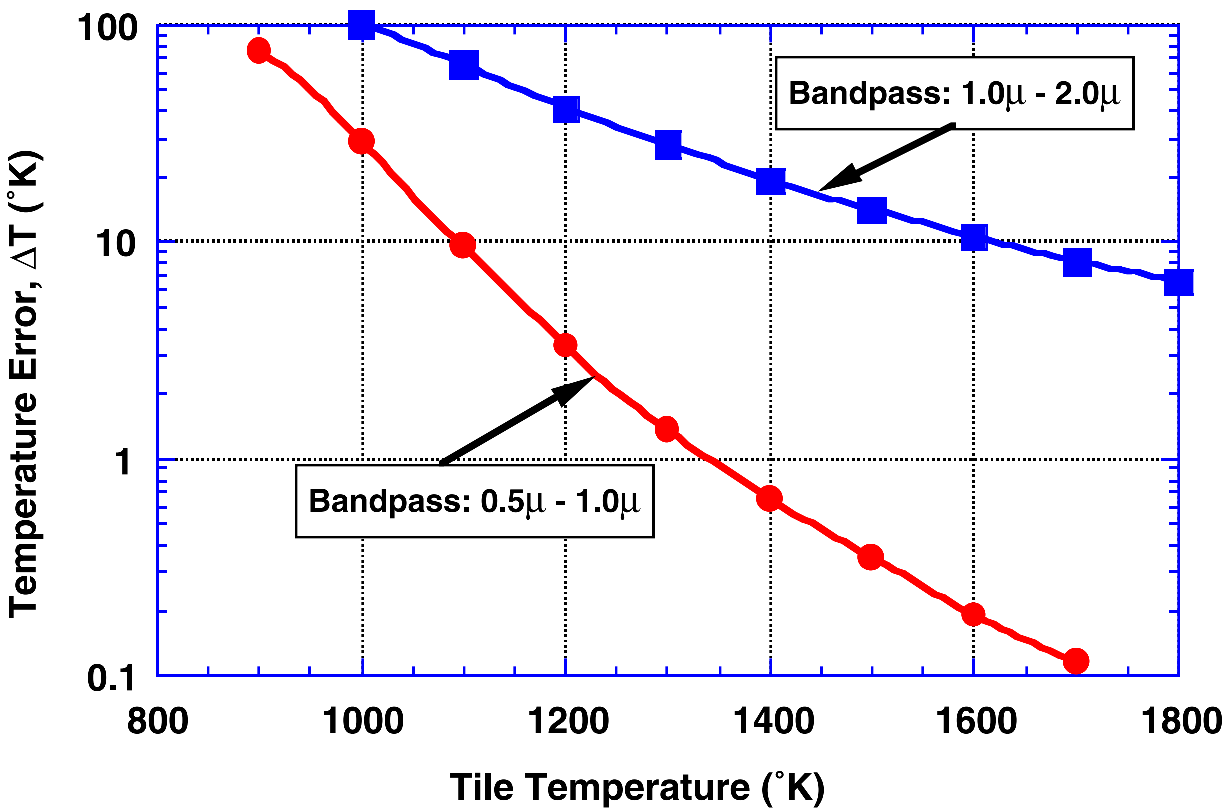

Fig. 4 Error in the tile temperature measurement due to heating of the Be mirrors for the noted band passes.

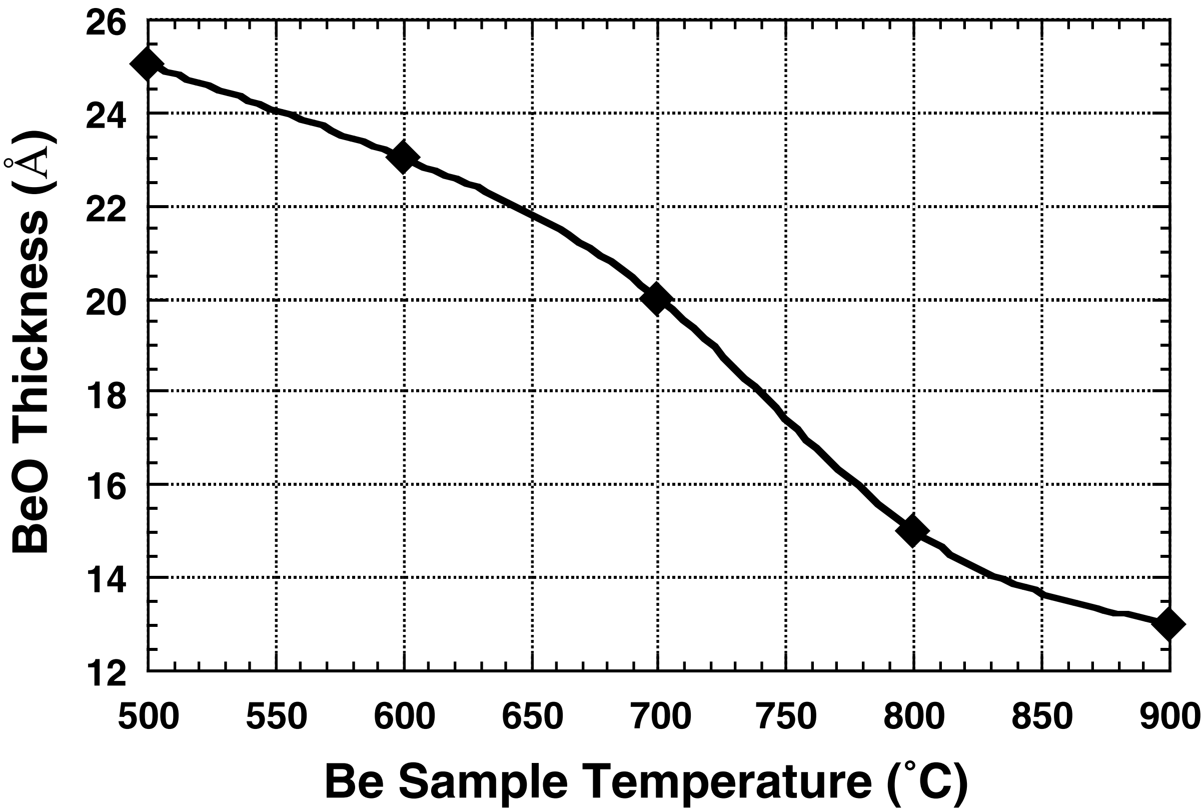

Fig. 5 BeO thickness as deduced from Auger ratio measurements as a function of Be sample temperature.